Automated Calibration of Temporal Changes in the Speed of Sound in Optoacoustic Tomography

Subhamoy Mandal[a,b], X Luís Deán-Ben[a,c] and Daniel Razansky[a,c]

[a]Institute for Biological and Medical Imaging, Helmholtz Center Munich,
[b]Faculty of Electrical Engineering and Information Technology, [c]Faculty of Medicine,
Technische Universität München, Munich, Germany

ABSTRACT

Reconstruction in multispectral optoacoustic tomography has become an critical area of importance, given the development of real-time imaging and visualization techniques. Speed of sound calibration is an intrinsic problem associated with the reconstruction process. Traditionally, the calibration has been user mediated, making it a tedious and offline affair. In this manuscript, we aim to introduce autofocusing and wavelet based measures to automatically calibrate the speed of sound. Further, it is observed that the temperature of the coupling medium (water) often drift during the signal acquisition, severely straining the image quality. The measures address these problems by iteratively determining the speeds with the changing boundary conditions with time.

Keywords: Optoacoustic tomography, photoacoustic tomography, wavelets, image analysis, speed of sound variations, image reconstruction

1. INTRODUCTION

Multispectral optoacoustic tomography (MSOT) has emerged as a powerful tool for high resolution visualization of optical contrast, enabled through its hybrid nature of optical excitation and acoustic detection. The technology benefits from both the versatile optical contrast and high(diffraction-limited) spatial resolution associated with low-scattering ultrasound waves as opposed to photon propagation.[1] Recent developments demonstrate the feasibility of volumetric imaging in real time at video-rate, opening new possibilities of the optoacoustic technology to image dynamic events.[2–4] Thereby, the reconstruction procedure becomes a critical issue to be able to visualize three dimensional structures in real-time, and achieving fast yet accurate reconstruction presents its challenges.

In most of the present scanning methods water is used as an interface or coupling medium between the scanning objects and ultrasound detectors. The protocols assume that temperature is uniform and constant throughout the experiment and the same is ensured by heating the water till the body temperature of the animals (or other scanning object). However, in practical experimental setups often the heating circuit is turned off during scanning to prevent formation of bubbles and water currents. This causes a temporal variation in the water temperature, which in turn changes the speed of sound (SOS)producing image artifacts during reconstructions.[5]Image quality in optoacoustic tomography is strongly conditioned by the reconstruction algorithms employed, and the SOS is an intrinsic parameter contributing to the same. During the experiment, it is observed that the variations in temperature of the medium (and the object) cause notable degradation of image qualities, if unaccounted for.

In this work, we illustrate the performance of a procedure to automatically calibrate the speed of sound by factoring for the reconstruction image quality, using contrast based focus measures. In practice, the speed of sound is commonly calibrated heuristically by choosing the best looking image, the value of the SOS (uniform) is taken from the same and applied to the entire data. The proposed method is effective in reducing the need of human intervention, and correct for temporal variations in speed of sound. The methods reported in this articles are useful in automatically accounting for these temporal changes changes in temperature and offer better reconstructed images by choosing the most suitable speed of sound. Further, these methods also ensures that we can correct for the temperature drifts automatically even after the acquisition of the signals.

Further author information: (Send correspondence to Subhamoy Mandal)
Subhamoy Mandal.: E-mail: s.mandal@tum.de, Daniel Razansky.:E-mail: dr@tum.de
IBMI, Helmholtz Zentrum München, Ingolstädter Landstraße 1, 85764 Neuherberg, Germany.

2. ALGORITHMS FOR AUTO-CALIBRATION OF SPEED OF SOUND

Standard optoacoustic reconstruction algorithms assume that the imaged sample corresponds to a uniform non attenuating acoustic material perfectly matched to the coupling medium (water).[6–9] Further, it is also assumed that the temperature of the water bath (and the object) is kept constant over the period of experimentation. While these assumptions are sometimes valid to model actual soft tissues, the tomographic reconstructions obtained with such algorithms are generally affected by reduced resolution, quantification errors and other artefacts. We analyzed the efficacy of iterative algorithms which reconstructs only selected frames and computes the signal to noise ratio (SNR) of the reconstructed images, and the focus measures to find out the most suitable SOS.[10,11] Assuming that the best SNR performance is achieved when the speed of sound is used for reconstruction is closest to the actual speed of sound, the most suitable speed of sound value at a given instant (and a given temperature) was speed of sound identified. Moreover, once calibrated using sparse frames, this fixed SOS value was utilized for full 3D reconstruction. Given the fact that change of temperature is also a function of time, this process was re-iterated over regular intervals, yielding a fair estimate of instantaneous SOS for real-time reconstruction. The best match for the SOS is achieved when the final reconstructed image is in sharp focus. Thus autofocusing algorithms are used, along with wavelet based methods of focusing.

2.1 Focus Measures

In literature, Brenner's[12] and Tenengrad's[13] focus measures are best performing among the traditional measures for optoacoustic images,[10] thus we use the same as a reference.
The Brenner's gradient is a provides a quantitative measure for image sharpness. It computed the difference between the pixel values and its neighbors 2 pixels away. Given $f_{x,y} = f(x, y)$ is the gray level intensity of a pixel at (x, y), the Brenner's gradient can be expressed as:

$$F_B = \sum_{x,y} (f_{x+2,y} - f_{x,y})^2 + (f_{x,y+2} - f_{x,y})^2 \tag{1}$$

The Tenengrad's gradient uses an edge detection based approach (sharper edges corresponds to higher frequencies). The gradient is determined by a convolution operation between the Sobel operator (and its transpose) with the image pixels. The same can be represented as:

$$F_T = \sum_{x,y} (g * f_{x,y})^2 + (g^T * f_{x,y})^2 \tag{2}$$

$$g = \begin{pmatrix} -1 & 0 & 1 \\ -2 & 0 & 2 \\ -1 & 0 & 1 \end{pmatrix} \tag{3}$$

The images were reconstructed with different speeds of sound between 1460m/s to 1600m/s and the focus measures were calculated.

2.2 Wavelet based Methods

Wavelets offers a fresh new outlook in computing the focused measure, we utilized the transform domain coefficients and subband entropy for the same[14].[15] Daubechies wavelets with 6 vanishing moments and 3 depths of decomposition performed optimal for the reconstructed phantom images. In the wavelet domain, the focus measure can be expressed as:

$$M_W = M_H^2 / M_L^2$$

where,

$$M_H^2 = \sum_{l=1}^{k} [\sum_{(x,y)\in LHl} W_{LHl}^2(x, y) + \sum_{(x,y)\in HLl} W_{HLl}^2(x, y) + \sum_{(x,y)\in HHl} W_{HHl}^2(x, y)]$$

and,

$$M_H^2 = \sum_{(x,y)\in LL} W_{LLk}^2(x,y) \tag{4}$$

LHI, HHI, HLI, LL are selected operator windows in designated subbands.
The wavelet based method was particularly useful as higher signal-to- noise (SNR) ratio can be obtained by choosing the appropriate subbands. The variance in entropy were computed on the selected subbands. The wavelet based focus measures provide performance equivalence to the best spatial domain operators but has less computational cost, and better depth resolutions.

3. EXPERIMENTAL SETUP

Two tissue-mimicking agar phantoms (1.3% agar powder by weight) were used in the experiments. To provide more uniform illumination, 1.2% by volume of Intralipid was added to the solution. In the first phantom black polyethylene microspheres with an approximately diameter of 200 μm (Cospheric BKPMS $180 - 210$ μm) were embedded (3 in number). In the second phantom we embedded a printed (on paper using laser printer with black ink)diagram of a kidney.

An 256 element MSOT system was used for the experiments, as described by Razansky et. al.[16] In the named system, output laser beam was shaped to attain ring-type uniform illumination on the surface of the phantoms. The laser source is an optical parametric oscillator (OPO) laser with 10 Hz pulse repetition and a tunable optical wavelength that was set to 720 nm in the experiments. An array of 256 cylindrically-focused array of immersion PZT transducers with a central frequency of 5 MHz and a focal length of 140 mm was employed to collect the optoacoustic signals, which were amplified and digitalized with a custom-made data acquisition system. The detector array offers a 272 degree angular coverage in a given slice of focus. Each of the signals was averaged 10 times and band-pass filtered with cut-off frequencies between 0.1 and 7 MHz. Further, for the phantom with embedded microspheres, the water temperature was varied between 41°C and 24.1°C during the acquisition. The signals were recorded at an interval of 0.5°C, along with the timing details; the total acquisition time was 2hrs 32 min. Image reconstruction was done with a universal back-projection algorithm.[17]

4. RESULTS

The effects of variations in speed of sound caused by the changes in the temperature of the water bath are clearly observed in figures (1-2). In figure 1 we see that the ideal SOS is 1520 m/s (Temperature = 27.5°C) and there are visible distortion for when the image is reconstructed with an incorrect value of SOS. In figure 2, when the temperature is = 40.1°C the ideal SOS is approximately 1550 m/s.

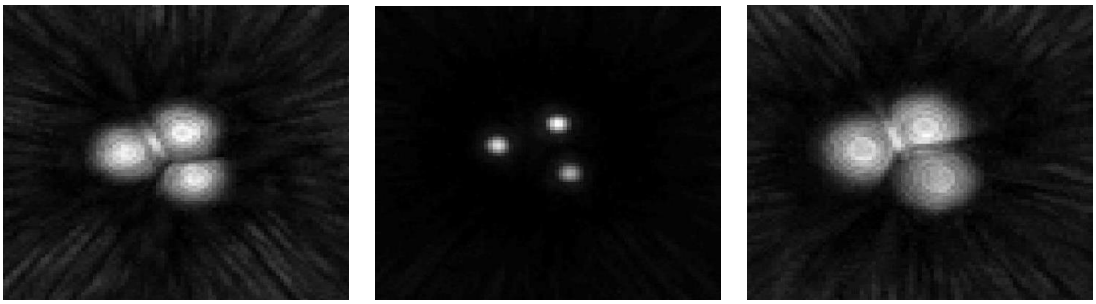

(a) 1480 m/s (b) 1520 m/s (c) 1560 m/s

Figure 1: Phantoms with microparticles- speed of sound (a-c) corrected against varying temperature with time; Temperature = 27.5°C, Calibrated speed of sound : 1520 m/s

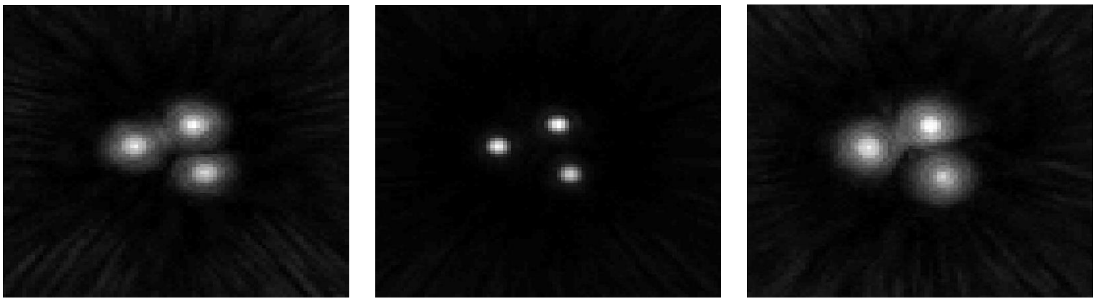

(a) 1520 m/s (b) 1550 m/s (c) 1580 m/s

Figure 2: Phantoms with microparticles- speed of sound (a-c) corrected against varying temperature with time; Temperature = 40.5°C, Calibrated speed of sound : 1550 m/s

We tested the algorithms on the phantom with embedded printed kidney shape, and used the autofocusing and wavelet measures for finding out the suitable SOS ($1558m/s \pm 4$m/s). The results are illustrated in figure 3; both the methods perform suitably good. Further, it is observed that Tenengrad's gradient performed better than the Brenner's gradient for this phantom. However, for phantom with microparticles the results from both the methods were similar.

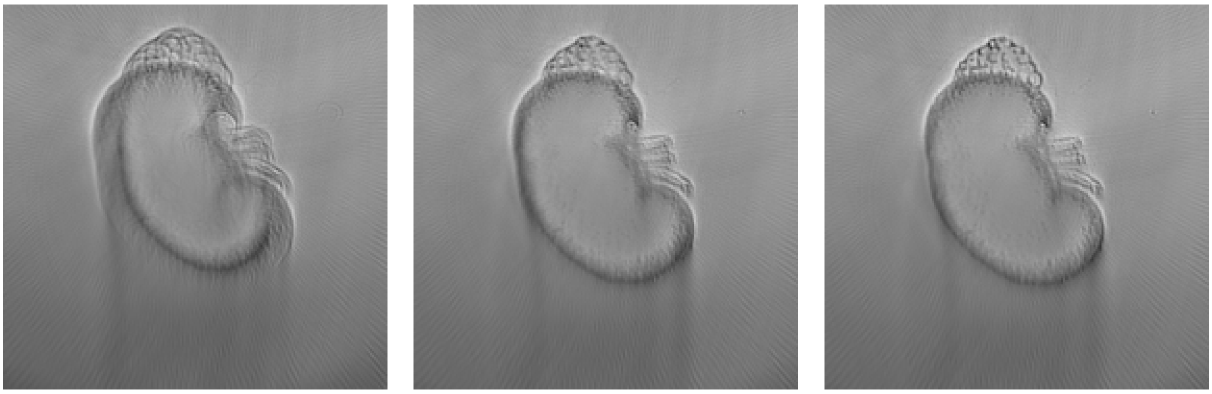

(a) Uncalibrated (b) Calibrated:Tenengrad Gradient (c) Calibrated:Wavelet Method

Figure 3: Phantom imaging in and out of plane: Auto-focusing algorithms are employed to choose the in-focus image (SOS:($1558m/s \pm 4$m/s) Temperature = 27.5°C)

5. CONCLUSIONS

Autofocusing algorithms were employed to achieve automatic speed of sound calibration for better reconstruction with varying temperature with time, and tested using tissue phantoms. A comprehensive experiment was conducted with drop in temperature of approximately 20°C over a time -frame of 142 minutes.It was observed that even a change of0.8°Ccaused a significant alteration of speed of sound thus affecting the quality of the reconstructed image. The failure to factor for these intra-scan variations in speed of sound causes image artifacts which impairs the structural information in the scans. Thus we can infer that changes in temperature of the coupling medium results in varying speed of sound which impacts the reconstruction algorithms (filtered back-projection) and the quality of the reconstructed image. Image analysis based speed of sound auto-calibration method can suitably be used for for better image reconstruction performance..

ACKNOWLEDGMENTS

Subhamoy Mandal acknowledges support (PhD Scholarship Award: A/11/75907)from the German Academic Exchange Service (DAAD). Daniel Razansky acknowledges support from the German Research Foundation (DFG) Research Grant (RA 1848/1) and the ERC Starting Independent Researcher Grant.

REFERENCES

[1] Razansky, D., "Multispectral optoacoustic tomography volumetric color hearing in real time," *Selected Topics in Quantum Electronics, IEEE Journal of* **18**(3), 1234–1243 (2012).

[2] Buehler, A., Deán-Ben, X. L., Claussen, J., Ntziachristos, V., and Razansky, D., "Three-dimensional optoacoustic tomography at video rate," *Opt. Express* **20**, 22712–22719 (Sep 2012).

[3] Buehler, A., Herzog, E., Razansky, D., and Ntziachristos, V., "Video rate optoacoustic tomography of mouse kidney perfusion," *Opt. Lett.* **35**, 2475–2477 (Jul 2010).

[4] Wang, B., Xiang, L., Jiang, M. S., Yang, J., Zhang, Q., Carney, P. R., and Jiang, H., "Photoacoustic tomography system for noninvasive real-time three-dimensional imaging of epilepsy," *Biomed. Opt. Express* **3**, 1427–1432 (Jun 2012).

[5] Van de Sompel, D., Sasportas, L. S., Dragulescu-Andrasi, A., Bohndiek, S., and Gambhir, S. S., "Improving image quality by accounting for changes in water temperature during a photoacoustic tomography scan," *PLoS ONE* **7**, e45337 (10 2012).

[6] Paltauf, G., Viator, J. A., Prahl, S. A., and Jacques, S. L., "Iterative reconstruction algorithm for optoacoustic imaging," *Journal of the Acoustical Society of America* **112**(4), 1536–1544 (2002).

[7] Norton, S. J. and Vo-Dinh, T., "Optoacoustic diffraction tomography: analysis of algorithms," *Journal of the Optical Society of America A* **20**(10), 1859–1866 (2003).

[8] Deán-Ben, X. L., Buehler, A., Ntziachristos, V., and Razansky, D., "Accurate model-based reconstruction algorithm for three-dimensional optoacoustic tomography," *IEEE Transactions on Medical Imaging* **31**(10), 1922–1928 (2012).

[9] Filbir, F., Hielscher, R., and Madych, W. R., "Reconstruction from circular and spherical mean data," *Applied and Computational Harmonic Analysis* **29**(1), 111–120 (2010).

[10] Treeby, B. E., Varslot, T. K., Zhang, E. Z., Laufer, J. G., and Beard, P. C., "Automatic sound speed selection in photoacoustic image reconstruction using an autofocus approach," *Journal of Biomedical Optics* **16**(9), 090501–090501–3 (2011).

[11] Garud, H., Ray, A., Mandal, S., Sheet, D., Mahadevappa, M., and Chatterjee, J., "Volume visualization approach for depth-of-field extension in digital pathology," in [*Image and Signal Processing (CISP), 2011 4th International Congress on*], **1**, 335–339 (2011).

[12] Santos, A., Ortiz de Solórzano, C., Vaquero, J., Peña, J., Malpica, N., and del Pozo, F., "Evaluation of autofocus functions in molecular cytogenetic analysis.," *J Microsc* **188 (Pt 3)** (1997).

[13] Pech-Pacheco, J. L., Cristobal, G., Chamorro-Martinez, J., and Fernandez-Valdivia, J., "Diatom autofocusing in brightfield microscopy: a comparative study," in [*Pattern Recognition, 2000. Proceedings. 15th International Conference on*], **3**, 314–317 vol.3 (2000).

[14] Pertuz, S., Puig, D., and Garcia, M. A., "Analysis of focus measure operators for shape-from-focus," *Pattern Recognition* **46**(5), 1415 – 1432 (2013).

[15] Xie, H., Rong, W., and Sun, L., "Wavelet-based focus measure and 3-d surface reconstruction method for microscopy images," in [*Intelligent Robots and Systems, 2006 IEEE/RSJ International Conference on*], 229–234 (2006).

[16] Razansky, D., Buehler, A., and Ntziachristos, V., "Volumetric real-time multispectral optoacoustic tomography of biomarkers," *Nature protocols* **6**(8), 1121–1129 (2011).

[17] Xu, Y. and Wang, L. V., "Effects of acoustic heterogeneity in breast thermoacoustic tomography," *IEEE Transactions on ultrasonics, ferroelectrics and frequency control* **50**(9), 1134–1146 (2003).